EARTH'S CRYOSPHERE
SCIENTIFIC JOURNAL

Earth`s Cryosphere, 2017, vol. XXI, No. 2, pp. 28–37 **http://earthcryosphere.ru/**

CRYOGENIC PROCESSES AND FORMATIONS

DOI: 10.21782/EC2541-9994-2017-1(28-37)

THERMODENUDATION ON YAMAL PENINSULA AS A SOURCE OF THE DISSOLVED ORGANIC MATTER INCREASE IN THAW LAKES

Yu.A. Dvornikov[1], M.O. Leibman[1,2], B. Heim[3], A.V. Khomutov[1,2], S. Roessler[4], A.A. Gubarkov[5]

[1] *Earth Cryosphere Institute, SB RAS, P/O box 1230, Tyumen, 625000, Russia; ydvornikow@gmail.com*
[2] *Tyumen State University, 6, Volodarskogo str., Tyumen, 625003, Russia*
[3] *Alfred Wegener Institute for Polar and Marine Research, 14473, Telegrafenberg A43, Potsdam, Germany*
[4] *FIELAX, 27568, Schleusenstr. 14, Bremerhaven, Germany*
[5] *Tyumen Industrial University, 38, Volodarskogo str., Tyumen, 625000, Russia*

This paper is devoted to the study of thermodenudation impact on concentration of dissolved organic matter in lake water. We present results of measured concentration of colored dissolved organic matter in water samples collected from the lakes in Central Yamal. We show the difference of colored dissolved organic matter concentration in lakes with thermo-denudational coasts and in intact lakes. Buried peat layers discovered in thermocirque exposures appeared to have high concentration of dissolved organic carbon. We found average concentration of colored dissolved organic matter 3.5–4.5 times higher in lakes with thermocirques than in intact lakes.

Colored dissolved organic matter, thermocirques, Yamal lakes

INTRODUCTION

After long storage in a perennially frozen state, the organic matter from peat layers accumulated during the Holocene Climate Optimum can repeatedly undergo biochemical cycles [*Vonk et al., 2013*] in the context of climatic changes observed in the Arctic in recent decades [*IPCC, 2014*]. Warming permafrost [*Romanovsky et al., 2010*] and resulting increase of active layer thickness (ALT) [*Zhang et al., 1997*] are capable to trigger the activation of cryogenic processes (thermo-denudation, cryogenic landslides) in Central Yamal [*Leibman and Kizyakov, 2007; Leibman et al., 2015*]. Thermo-denudation is associated with bodies of tabular ground ice occurring rather close to the surface [*Parmuzin and Sukhodolskii, 1982; Dubikov, 2002; Leibman and Kizyakov, 2007; Badu, 2013*]. Formation of themocirques and retrogressive thaw slumps as a result of tabular ground ice thaw may cause alterations in geochemistry of the lakes with thermo-denudational coast [*Kokelj et al., 2005*]. Lakes represent natural reservoirs providing conditions for accumulation of organic matter after its transport from the surrounding catchments and therefore can serve as an intrinsic indicator of landscape changes in the Arctic.

Cryogenic translational landslides were the main focus of field research in Central Yamal ("Vaskiny Dachi" research station) during the period of observations commenced in 1987 [*Leibman and Kizyakov, 2007*]. Thermocirques adjacent to lakes were rare in the area and small in size. Four thermocirques were known, two of them ceased to exist after tabular ground ice exhausted due to continuous thaw, while the remaining two experienced periodical attenuation [*Leibman, 2005*].

In the period spanning from spring 2012 to fall 2013, an activation of thermo-denudation could be seen [*Leibman et al., 2015*] due to the dramatic increase in summer air temperature and associated ALT deepening. At least six thermocirques were found to have formed on lake coastal zones in the summers of 2012 and 2013 (Fig. 1), which prompted the transport of a considerable amount of detached material downslope making thereby its significant contribution to lake water. Besides mineral components, this material also included both dissolved and particulate organic matter.

The colored fraction of dissolved organic matter (CDOM) is an essential component of aquatic ecosystems [*Kalle, 1939; Skopintsev, 1950*], including those of high-latitude Arctic lakes [*Vincent et al., 1998*]. CDOM is dominantly composed of humic and fulvic acids [*Skopintsev, 1950; Wetzel, 2001*].

CDOM, being a major component of dissolved organic carbon (DOC), acts as a measurable parameter of the organic content in surface waters. CDOM absorbing primarily short wavelength light (UV and

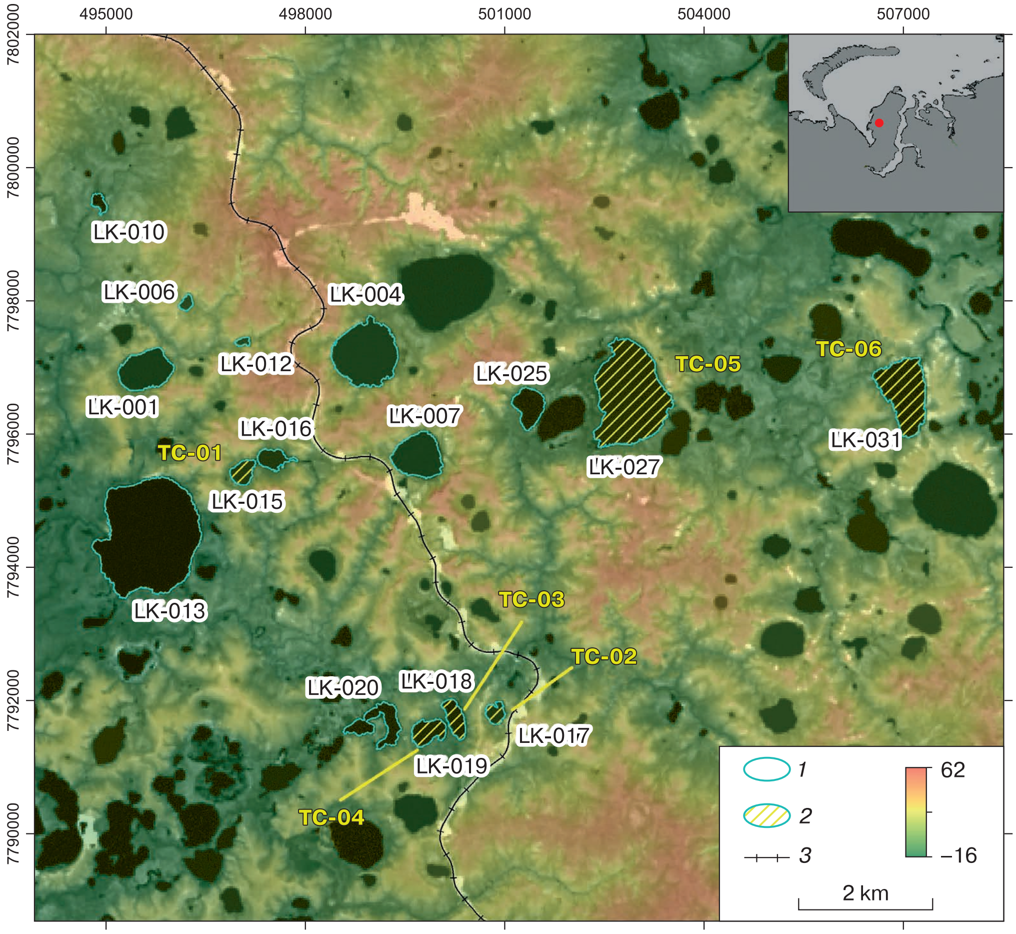

Fig. 1. Schematic map of field points at the key site ("Vaskiny Dachi" research station).

1 – study lakes; *2* – study lakes with thermocirques in coastal zone (TC – thermocirque index, LK – lake index); *3* – Obskaya – Bovanenkovo railroad. Base map: Landsat 8 image dated 19.07.2014 (NIR band) and DEM TanDEM-X (DLR©) with 12 m spatial resolution (elevations are equated to a.s.l.; the Baltic system of heights). Coordinates are given in UTM Projection, zone 42N.

blue wavelength ranges of the electromagnetic spectrum) has a considerable influence on the depth of the solar radiation penetrating into water of lakes/ponds, and on their temperature regime [*Zaneveld, 1975; Vincent and Pienitz, 1996; Twardowski and Donaghay, 2001*]. CDOM serves as an indicator of lake color [*Gjessing, 1976*] and optically measurable proxy of DOC.

Dissolved organic matter (DOM) in water column can be of autochthonous and allochthonous types of aquatic humic and fulvic matter [*Kalle, 1966*]. Autochthonous DOM is a product of life activity of phytoplankton, while allochthonous DOM is transported to water bodies from the surrounding catchments. Given the unfavorable climatic conditions for abundant phytoplankton in northern high-latitude lakes, the autochthonous DOM does not appear a determining factor in the formation of cumulative DOC concentration there, while the allochthonous DOM may constitute the bulk of DOC concentration [*Engstrom, 1987; Wetzel, 2001*].

STUDY AREA

The "Vaskiny Dachi" research station is located at the Se-Yakha and Mordy-Yakha river basins in Central Yamal (70°17′ N, 68°53′ E, Fig. 1).

The limnicity of the key site is 12 %, which is close to the average value (10 %) for the whole peninsula [*Trofimov, 1975*] and can reach 20 % on the floodplains of the Se-Yakha and Mordy-Yakha rivers [*Romanenko, 1999*]. The abundance of khasyreys in the floodplain is, conversely, uncharacteristic of the Salekhardskaya (V^{th}) and Kazantsevskaya (IV^{th}) geomorphological terraces composed of marine sediments. The lake area ranges from 0.14 to 346.6 hectares, averaging 11.1 ha.

The lake catchments delivering material into the surface waters of streams, rivers, ponds and lakes exhibit a range of terrain conditions. The lithological composition of the upper layer of lake catchments is represented by sands and clays that typify Salekhardskaya (V^{th}), Kazantsevskaya (IV^{th}) and the Third

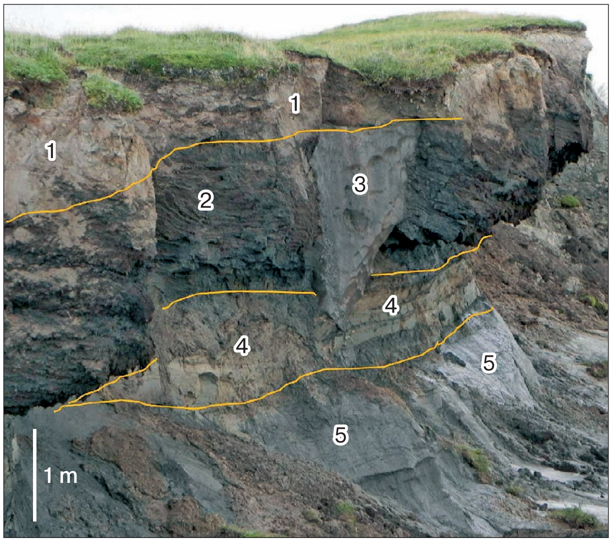

Fig. 2. TC-01 thermocirque exposure and its cryolithological structure:

1 – sandy-loamy slope deposits; 2 – peat; 3 – ice wedges; 4 – interbedding of sand, loam and clay; 5 – tabular ground ice. Photo by M.O. Leibman.

(IIIrd) geomorphological terraces. The vegetation cover is dominated by sedge communities, shrubs, dwarf-shrubs, and mosses [*Rebristaya and Khitun, 1998*].

We started to measure DOM concentration in the lake water when thermocirques began to actively form, exposing permafrost and ground ice in their side walls. The exposures encountered during the 2012–2015 field campaigns comprised buried ice-wedges intervening into tabular ground ice (Fig. 2). We found also buried peat layers with thickness of a few meters (Fig. 2) and mineral horizons enriched by organic matter.

METHODS

Water samples were collected in August–September during the 2014–2015 field campaigns of the Earth Cryosphere Institute SB RAS. We carried out the monitoring of thermocirques activation and their further development.

Water sampling. Water was sampled under calm conditions from the upper 30 cm of the water column, either from the shore or from the boat at the center of lake. Samples were kept cool (4–8 °C) in the dark, to preclude the UV-induced photochemical transformation of the organic matter [*Bricaud et al., 1981*]. Samples were filtered using Whatman© GF/F glass-fiber filters with 0.7 μm pore size directly in the field.

A total of 34 samples from 17 lakes collected and analyzed in 2014 and repeatedly in 2015 are presented in this paper.

Water sample analysis. Laboratory measurements of CDOM concentration in water samples were carried out at the Otto Schmidt Laboratory in St. Petersburg. Absorption of the dissolved fraction was measured using a dual-beam spectrophotometer Specord© 200 between 200 and 750 nm (UV/Vis spectra) with spectral resolution of 1 nm, which allowed to determine absorption spectra in each sample.

To calculate the CDOM absorption value $a(\lambda)$ the measured absorbance ($A = -\lg I/I_0$) was normalized to natural logarithm with multiplying by 2.303 and normalized to the cuvette length by dividing it by the length of the cuvette [*Davies-Colley and Vant, 1987*] through which the light was transmitted:

$$a(\lambda)_{\mathrm{CDOM}} = 2.303\frac{-\lg\left(I/I_0\right)}{L}, \tag{1}$$

where I is the measured light intensity after passing the cuvette; I_0 is the initial light intensity generated by the lamp; L is the light path length equal to the cuvette length). In this study, we use 0.05 and 0.10 m long quartz cuvettes. The absorption measurement error constitutes ±0.002 m^{-1}.

All the absorption spectra $a(\lambda)_{\mathrm{CDOM}}$ were corrected for scattering by subtracting the absorption value at 700 nm, where it is taken equal to zero [*Davies-Colley and Vant, 1987; Twardowski et al., 2004*], from the full spectra.

Absorption $a(\lambda)_{\mathrm{CDOM}}$ measured in m^{-1} is found to be directly proportional to organic matter (fulvic and humic acids) concentration in water [*Skopintsev, 1950*]. Spectral slopes (i.e. the spectral shape of the absorption) of absorption values ($S(\lambda)$, nm^{-1}) were calculated from the CDOM absorption spectra over the wavelength range between 350 и 500 nm. The $S(\lambda)$ parameter characterizes the curvature of the spectral slope of CDOM indicating the source and properties of organic matter [*Davies-Colley and Vant, 1987; Carder et al., 1989; Blough and Green, 1995; Helms et al., 2008*].

Absorption values tend to exponentially decrease with growing wavelength [*Jerlov, 1968*]. The CDOM absorption spectrum can be reconstructed from $a(\lambda)_{\mathrm{CDOM}}$ and $S(\lambda)$ values [*Bricaud et al., 1981*].

Monitoring of thermocirques. During the 2012–2015 field campaigns we monitored thermo-denudation forms, thermocirques (Fig. 3). Descriptions of the sections were supplemented by the thermocirque cliff-top retreat rate monitoring using GPS+GLONASS equipment, and high-resolution satellite images GeoEye-1 (05.07.2013), GeoEye-1 (15.08.2009) and QuickBird (30.07.2010). The images were provided by Digital Globe Foundation©. GPS-receivers employed in the study are: Garmin© Dakota 20, 60, Etrex 30 (measurement error in plan ±1 m) and Trimble© 5700 (measurement error: ±0.1 m). The receiver was placed directly above the thermocirque cliff-top line.

Fig. 3. Photographs of thermocirque TC-01.
a – September 2012; *b* – August 2015. Photos by A.V. Khomutov. Thermocirque location is shown in Fig. 1.

Multispectral images with enhanced spatial resolution were obtained using the PANSHARP2 fusion algorithm provided by the PCI Geomatica 2014 software (PCI Geomatics©) [*Zhang, 2004*]. This fusion algorithm has been successfully tested on very high spatial resolution images [*Du et al., 2007*].

The images were orthorectified using the OrthoEngine© module within the PCI Geomatica 2014 software. In August 2014, the precise coordinates of seven reference points including the Obskaya–Bovanenkovo railway objects, bridges, and buildings, were determined using a differential GPS receiver Trimble© 5700.

These points were bundled together with 40 tie points, to enable the precise image stacking with each other (RMSE are 0.46, 0.37, 0.57 for the GeoEye-1 2009, GeoEye-2013, QuickBird 2010 images respectively). The orthorectification was based on TanDEM-X© IDEM digital elevation model (DEM) with a spatial resolution of 12 m.

RESULTS

Analysis of water samples. Table 1 represents the results of water sample analyses. The absorption values measured at wavelength of 440 nm ($a(440)_{CDOM}$) vary from 0.736 to 8 m^{-1} and from 0.58 to 8 m^{-1} for 2014 and 2015, respectively (Table 1). The lowest values are found in the lakes LK-025

Table 1. **Results of tests for water samples taken from lakes (LK) (Fig. 1) and thermocirques (TC)**

Lake index	$a(440)_{CDOM}$, m^{-1}		$S(350–500)$, nm^{-1}		TC index
	2014	2015	2014	2015	
LK-001	0.818	0.640	0.016 54	0.016 76	–
LK-004	1.189	0.735	0.016 48	0.016 58	–
LK-006	2.359	2.531	0.018 17	0.017 50	–
LK-007	1.351	0.854	0.016 59	0.017 14	–
LK-008	3.820	0.580	0.014 07	0.018 58	–
LK-010	1.711	2.272	0.017 21	0.017 52	–
LK-012	2.300	2.588	0.018 05	0.018 30	–
LK-013	5.015	7.849	0.015 33	0.014 54	–
LK-015	6.338	4.940	0.013 55	0.014 58	TC-01
LK-016	4.179	3.049	0.016 17	0.016 92	–
LK-017	4.640	1.797	0.013 21	0.015 25	TC -02
LK-018	5.458	4.808	0.014 36	0.014 67	TC -03
LK-019	7.651	6.330	0.013 33	0.014 58	TC -04
LK-020	1.722	1.095	0.015 66	0.016 50	–
LK-025	0.736	0.713	0.018 33	0.017 53	–
LK-027	2.386	1.080	0.013 82	0.015 94	TC -05
LK-031	8.000	8.000	0.011 74	0.013 21	TC -06
Average	*3.5*	*2.9*	*0.0154*	*0.0162*	

Note. $a(440)_{CDOM}$ is CDOM spectral absorption at 440 nm wavelength, $S(350–500)$ is spectral slope parameter in the visible region of the spectrum (350–500 nm).

Table 2. **Parameters of thermocirques (TC) (location can be seen on Fig. 1)**

TC index	Disturbed area*, ha	Average retreat rate of the cliff-top**, m/year	Class of object	Year of activation
TC-01	0.68	6.6	Natural	2012
TC-02	0.81	4.1	Technogenic	Earlier than 2010
TC-03	0.53	8.7	Natural	2012
TC-04	1.02	10.4	Natural	2012
TC-05	–	7.6	Natural	2012
TC-06	3.98	18.5	Natural	2012

* In 2015.
** Over the period of 2012–2015.

(2014) and LK-008 (2015), while the highest value belongs to lake LK-031 for both years (Fig. 1, Table 1).

The year 2015 was generally characterized by lower CDOM concentrations in lakes (average 2.93 m^{-1}) compared to 2014 (average 3.51 m^{-1}). Out of all 17 lakes only 4 (LK-006, LK-010, LK-012, LK-013) showed an increase in $a(440)_{CDOM}$. The highest values for both years belong to lakes with thermocirques. In addition, LK-013 (the only lake on Mordy-Yakha river floodplain) has high $a(440)_{CDOM}$ value.

The absorption in spectral slopes $S(350–500)$ vary from 0.0117 to 0.0183 nm^{-1} and from 0.0132 to 0.0186 nm^{-1} for 2014 and 2015, respectively (Table 1). The lowest value is attributed to lake LK-031, whereas the highest corresponds to lakes LK-025 and LK-008 (Fig. 1) for 2014 and 2015, respectively. The year 2015 showed higher values of $S(350–500)$ for lakes (average 0.0162 nm^{-1}) compared to 2014 (average 0.0154 nm^{-1}). Out of 17 lakes only 3 (LK-006, LK-013, LK-025) were marked by reduced $S(350–500)$ values in 2015. The lakes with thermo-denudational coasts were characterized by the lowest $S(350–500)$ values in both years of observation, except for lakes LK-008 (2014) and LK-013 (2015) (Fig. 1) also characterized by low $S(350-500)$ values (Table 1).

Results of the thermocirque monitoring. Table 2 shows quantitative parameters of the development of thermocirques (Fig. 1). The thermocirque cliff-top retreat rates range between 4.1 and 18.5 m/year (Table 2, Fig. 4). The width of thermocirques can reach 200 m, with their area ranging from 0.53 to 3.98 ha (Table 2, Fig. 4).

DISCUSSION

CDOM parameters in Yamal lakes. High-latitude inland water bodies north of the tree-line are characterized by low concentrations of CDOM [*Vincent et al., 1998*], which tend to decrease farther north of the forest-tundra limits [*Vincent and Pienitz, 1996*]. However, the area of Central Yamal is characterized by the presence of high (up to 2 m) willow shrubs [*Rebristaya and Khitun, 1998; Ukraintseva, 1998; Leibman, 2004*], which occupy primarily topographic depressions, concave and wind-protected leeward slopes.

Owing to decomposition of the leaf litter, high willow shrubs have more biomass to produce larger amount of organic matter, than zonal tundra plants. This organic matter becomes a source of allochthonous CDOM in the lake water in addition to CDOM seasonally arriving from the thawing ALT [*Vonk et al., 2013*].

Import of organic matter from the catchments is largely governed by surface washout by liquid precipitation, as well as by intensive snowmelt [*Chistov, 1991*], given the substantial snow reserves in the study region [*Dvornikov et al., 2015*]. The organic matter transport processes are not discussed in detail in this paper due to its specific focus on the relationship between activation of thermocirques and CDOM concentration in the lake water.

We compared CDOM concentrations in lakes of Central Yamal and in lakes located in more southerly regions. Values for spectral absorption in the literature are given over diverse wavelengths, therefore these values were re-calculated to 440 nm using the equation 2 [*Bricaud et al., 1981*]

$$a(440)_{CDOM} = a(\lambda_g)_{CDOM} \exp[-S(440 - \lambda_g)], \quad (2)$$

where $a(\lambda_g)_{CDOM}$ is absorption at a particular wavelength λ_g found in the related publication; S is the spectral slope in the UV-visible wavelengths (350–500 nm), which is assumed to be on average 0.015 nm^{-1}, found for inland and sea waters [*Twardowski et al., 2004*], as well as measured in the lakes in Central Yamal (Table 1).

Average spectral absorption of CDOM at 440 nm measured in lakes of Central Yamal (Table 1) range between 2.93 and 3.51 m^{-1}, which is comparable, due to increased additional input of allochthonous CDOM to the Yamal lakes, with values measured in lakes of southern Sweden and Finland (4–5 m^{-1}) [*Kutser et al., 2005*].

The $a(440)_{CDOM}$ average values measured in the Kolyma and other rivers of Eastern Siberia in July 2008 and 2009 (2.00 ± 0.92 m^{-1}) [*Griffin et al., 2011*] are interpreted to be within the same limits as in the Central Yamal lakes. The higher concentrations of CDOM (mostly allochthonous) measured by J. Breton and others in 15 shallow bogs in the Canadian Sub-Arctic (average spectral absorption values: 6.76 ± 5.04 m^{-1}), are accounted for the terrestrial input from the surrounding catchments [*Breton et al., 2009*]. We have also measured CDOM absorption in 10 small water bodies (thaw ponds with area less than 1000 m^2), similar in size to those described in [*Breton*

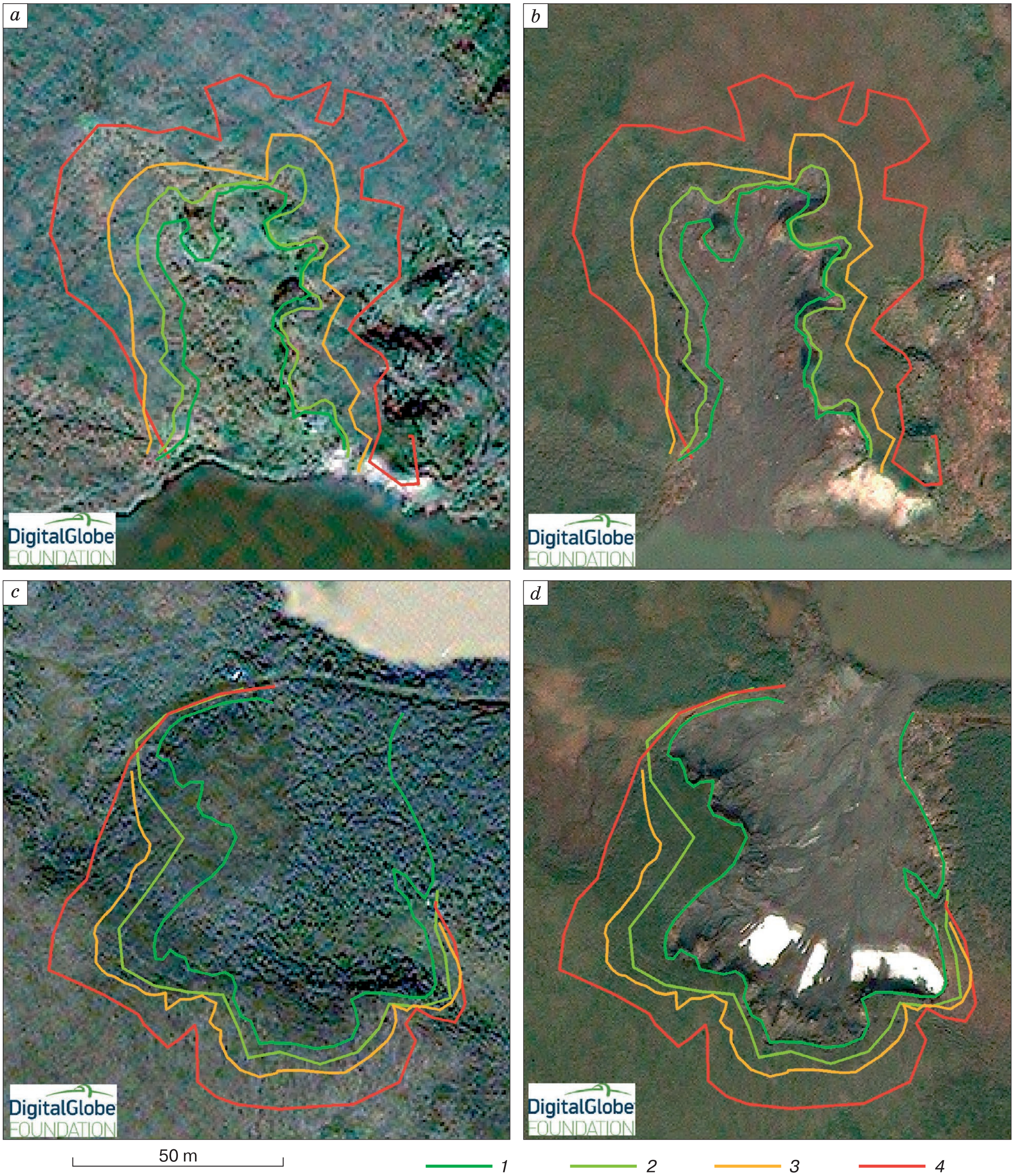

Fig. 4. The state of lake coastal zones before (*a*, *c*) and after (*b*, *d*) formation of thermocirques (TC).

a, *c* – QuickBird image dated 30.07.2010 with 0.6 m resoliution; *b*, *d* – GeoEye-1 dated 05.07.2013 at 0.5 m resolution. Thermocirque dynamics: *a*, *b* – TC-01; *c*, *d* – TC-04. Thermocirque cliff-top position: *1* – 05.09.2012 (*a*, *b*), 05.07.2013 (*c*, *d*); *2* – 05.07.2013 (*a*, *b*), 28.08.2013 (*c*, *d*); *3* – 27.08.2013 (*a*, *b*), 27.08.2014 (*c*, *d*); *4* – 21.08.2015 (*a*, *b*), 26.08.2015 (*c*, *d*). Thermocirque cliff-top position determined with the use of: *1*, *3* (*a*, *b*) – Garmin 60 GPS receiver; *1* (*c*, *d*), *2* (*a*, *b*) – GeoEye-1 image dated 05.07.2013; *2* (*c*, *d*), *4* – Garmin Etrex 30 GPS+GLONASS receiver; *3* (*c*, *d*) – DGPS- Trimble GNSS 5700 receiver.

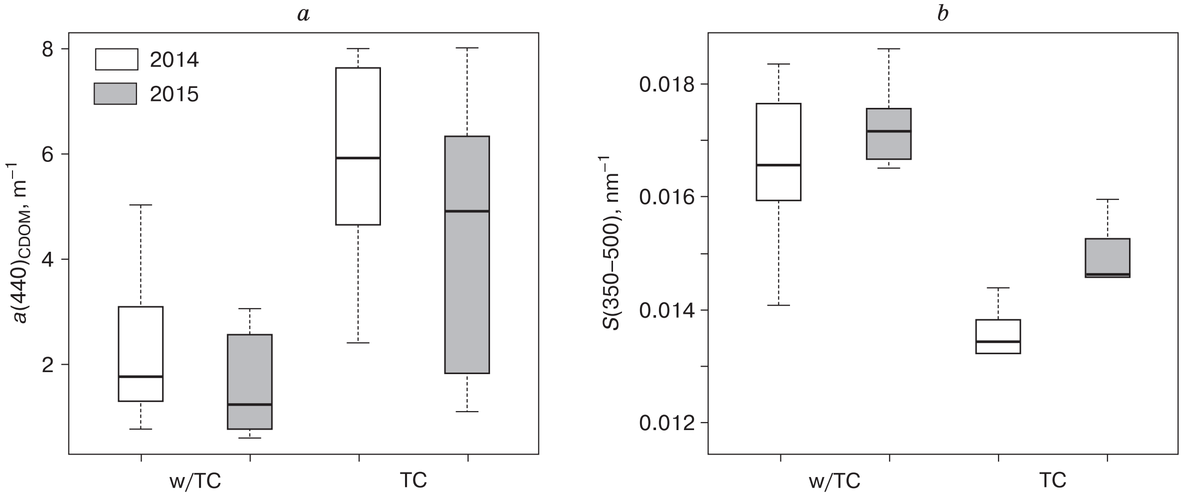

Fig. 5. Differences in $a(440)_{CDOM}$ values (a) and spectral slope $S(350–500)$ (b) in intact lakes (w/TC) and with active thermocirques (TC).

et al., 2009]. Its values are also higher than average for lakes (4.6 ± 4.5 m^{-1}).

Input of allochthonous CDOM leads to a decrease slope values (*S*) [*Laurion et al., 1997*]. The *S* measurements were found approximately within the same wavelength range (0.0135–0.0186 nm^{-1}, average 0.0158 nm^{-1}) for lakes located in both the Canadian Sub-Arctic and in Central Yamal (Table 1).

Relationship between CDOM parameters and thermocirques discharging into the lakes. S. Kokelj and others describe that thermokarst lakes with retrogressive thaw slumps in the coastal zone in the Mackenzie river delta generally have a lower DOC concentration and water in such lakes is characterized by higher transparency [*Kokelj et al., 2005*]. In [*Thompson et al., 2008; Kokelj et al., 2009*], this is associated with the organic matter sedimentation on clay particles (i.e. adsorption of organic material by clayey particles) and their joint settling to the lake bottom (when thermodenudation is still active). In these studies, at the time of sampling only a very few of retrogressive thaw slumps were active and accompanied by the transport of material [*Kokelj et al., 2009*].

Table 3. **Increase in CDOM concentration resulting from thermocirque (TC) activation in the coastal zone of four lakes**

Lake index	$a(440)_{CDOM}$, m^{-1}		Augmentation, %
	2009	2013	
LK-015	1.277	5.265	312
LK-027	0.528	2.664	404
LK-178*	2.329	9.371	302
LK-298**	1.078	7.444	590

* 5.7 km N–NE of lake LK-004.
** 0.5 km N of lake LK-025.

According to our field observations, the thermocirques activated mainly in 2012 [*Leibman et al., 2015*], which allows to assess them as relatively young. They continued to actively develop until 2015 [*Khomutov et al., 2016*].

Buried peat lenses with a characteristic smell of decomposing organic matter were encountered in the sections of newly formed thermocirques, being a source of additional input of the allochthonous organic matter (Fig. 2). The measured DOC concentration in the filtered peat-water sample constituted 243 mg/L, which is 50 times higher than DOC in lakes of Central Yamal. Activation of thermocirques may launch the organic matter export in large amounts to the lakes from perennially frozen peat lenses.

The 2014 and 2015 field data analyses conducted separately for intact lakes and for lakes with thermocirques have shown that the median CDOM absorption values at 440 nm wavelength in lakes with thermo-denudational coasts is 3.5 times (2014) and 4.4 times (2015) higher than in intact lakes (without thermocirques) (Fig. 5, *a*). It can be interpreted as follows: *at an early stage, thermo-denudation processes at the lake coasts lead to a significant increase in CDOM concentration in those lakes.*

The data obtained confirm that lakes with thermocirques tend to have lower *S* values (0.0134 and 0.0146 nm^{-1} for 2014 and 2015, respectively) compared to intact lakes (0.0165 nm^{-1} for 2014 and 0.0171 nm^{-1} for 2015) (Fig. 5, *b*).

The atmospheric-corrected GeoEye-1 images of 2009 and 2013 and application of the algorithm for remote estimation of $a(440)_{CDOM}$ parameter [*Kutser et al., 2005; Dvornikov et al., 2014, 2016*] enabled us to estimate the change in CDOM concentration in lakes in 2013, when active thermocirques not existent at the time of the 2009 acquisition, came on the scene.

Table 3 shows the results of CDOM absorption values at wavelength 440 nm retrieved from satellite images taken in 2009 and 2013. The coverage of images allowed to analyze 4 lakes only. Compared to 2009, the concentration of CDOM has shown a 4–7-fold increase, from 312 to 590 %, in 2013 (Table 3).

CONCLUSIONS

The paper presents quantitative characteristics of the development of thermo-denudation landforms (thermocirques) which appeared in the summer 2012, and the related variation in CDOM concentration and S values for intact lakes and lakes with thermo-denudation coasts using field data complemented by laboratory analyses and remote sensing data processing.

1. Thermocirque cliff-top retreat at a rate of 4.1 to 18.5 m/year, with some of the thermocirques gaining up to 200 m in width; their area varies from 0.53 to 3.98 ha.

2. Large peat lenses were found in the exposures of thermocirque walls. The concentration of dissolved organic carbon (DOC) in the filtered peat-water sample from one of peat lenses was as high as 243 mg/L, while average concentration of DOC in the Yamal lakes constitutes 4–5 mg/L.

3. In lakes with thermo-denudation coasts, concentration of the colored dissolved organic matter (CDOM) is higher than in the intact lakes. For lakes with thermocirques the mean values of $a(440)_{CDOM}$ range between 5.9 and 4.9 m^{-1} for 2014 and 2015, respectively. In case of intact lakes, these values are 3.5 and 4.4 times lower (1.7 and 1.1 m^{-1} for 2014 and 2015 respectively).

4. The properties of the organic matter exported from thermocirque walls differ from allochthonous organic matter arrived from surrounding catchments. Calculations of the spectral slope $S(350–500)$ for water sampled in 2014 and 2015 showed that the median values for lakes with thermodenudation coasts are 0.0134 and 0.0146 nm^{-1} respectively, while for lakes with intact coasts they equaled 0.0165 and 0.0171 nm^{-1}.

5. A significant (locally, 7-fold) increase in the CDOM concentrations in lakes can occur subsequent to the formation of thermocirques along the coastal zones. Additional analysis based on the remote sensing data with very-high spatial resolution allowed obtaining $a(440)_{CDOM}$ values for four lakes (2009) which coastal zones remained stable until 2012. It was followed by the observational data from 2013, when their coastal zones were already affected by thermocirques. The $a(440)_{CDOM}$ values have shown a 4.1–6.9-fold increase (on average, by 5.1 times) during the period from 2009 to 2013.

It has been shown that the activation of thermo-denudation on the Yamal peninsula is capable to trigger mobilization of the perennially frozen organic matter from ancient peat lenses and, ultimately, its transport into the lakes.

The authors thank the colleagues from Otto Schmidt Laboratory (Saint-Petersburg, Russia) – T.V. Skorospekhova, E.D. Dobrotina, I.V. Fedorova, N.K. Shumskaya, A.A. Chetverova for assisting in the laboratory analyses; A.K. Il'yasov from Lomonosov Moscow State University – for geodetic equipment; colleagues from the University of Alaska Fairbanks (UAF) and Digital Globe Foundation – for providing the remote sensing data. Authors also express their sincere appreciation to German Academic Exchange Service (DAAD) and the Helmholz Graduate School for Polar and Marine Research (POLMAR) for financial support.

The study was done within the scope of International projects: CALM and TSP; ONZ -12 "Processes in atmosphere and cryosphere as a control of the environmental changes"; and is partially supported by RFBR (Grant No. 13-05-91001-ANF_a); Russian Science Foundation Grant 16-17-10203, BMBF (Grant No. OSL-15-04); with support from The Presidential Council for grants, Science School Grant No. 9880.2016.5. The expeditions were organized with a support of Interregional Expedition Center "Arctic".

References

Badu, Yu.B., Gafarov, N.A., Podborny, E.E. (Eds.), 2013. Cryosphere of oil and gas condensate fields of Yamal Peninsula. OOO "Gazprom Expo", Moscow, 424 pp. (in Russian)

Blough, N.V., Green, S.A., 1995. Spectroscopic characterization and remote sensing of non-living organic matter, in: Zepp, R.G., Sonntag, C. (Eds.). The Dahlem Workshop on the Role of Nonliving Organic Matter in the Earth's Carbon Cycle. Wiley, Berlin, New York, pp. 23–45.

Breton, J., Valliere, C., Laurion, I., 2009. Limnological properties of permafrost thaw ponds in northeastern Canada. Can J. Fish Aquat. Sci., No. 66, 1635–1648, DOI: 10.1139/f09-108.

Bricaud, A., Morel, A., Prieur, L., 1981. Absorption by dissolved organic matter of the sea (yellow substance) in the UV and visible domains. Limnol. Oceanogr., No. 26, 43–53.

Carder, K.L., Steward, R.G., Harvey, G.R., Ortner, P.B., 1989. Marine humic and fulvic acids: Their effects on remote sensing of ocean chlorophyll. Limnol. Oceanogr., No. 34, 68–81.

Chistov, S.V., 1991. Determination principles of the environmental protection measures for landscapes of West-Siberian Arctic and Subarctic under economic development, in: Problemy ekologii polyarnykh oblastei (Ecological problems of polar regions). Ser. Sovr. probl. biosfery. Nauka, Moscow, pp. 29–35. (in Russain)

Davies-Colley, R.J., Vant, W.N., 1987. Absorption of light by yellow substance in freshwater lakes. Limnol. Oceanogr., No. 32, 416–425.

Dvornikov, Yu., Bartsch, A., Khomutov, A., et al., 2014. Process of organic transport in lakes of the Yamal region (POLYAR), in: Proc. of Arctic Change (Ottawa, Canada, 8–12 December, 2014): Oral Presentation Abstr. Ottawa, p. 56.

Dvornikov, Y.A., Khomutov, A.V., Mullanurov, D.R., et al., 2015. GIS and field data-based modelling of snow water equivalent in shrub tundra. Fennia, No. 193 (1), 53–65.

Dvornikov, Y., Leibman, M., Heim, B., et al., 2016. Geodatabase and WebGIS project for long-term permafrost monitoring at the Vaskiny Dachi research station, Yamal, Russia. Polarforschung, 85 (2), 107–115.

Du, Q., Younan, N.H., King, R., Shah, V., 2007. On the performance evaluation of pan-sharpening techniques. IEEE Geosci. and Remote Sensing Lett., No. 4 (4), 518–522.

Dubikov, G.I. (Ed.), 2002. Composition and Cryogenic Structure of Permafrost in Western Siberia. GEOS, Moscow, 246 pp. (in Russian)

Engstrom, D.R., 1987. Influence of vegetation and hydrology on the humus budgets of Labrador lakes. Can. J. Fish. Aquat. Sci., No. 44, 1306–1314.

Gjessing, E.T., 1976. Physical and chemical characteristics of aquatic humus. Annales Arbor Science Publ., Michigan, USA, 120 pp.

Griffin, C.G., Frey, K.E., Rogan, J., Holmes, R.M., 2011. Spatial and interannual variability of dissolved organic matter in the Kolyma River, East Siberia, observed using satellite imagery. J. Geophys. Res., No. 16, G03018, DOI: 10.1029/2010JG001634.

Helms, J.R., Stubbins, A., Ritchie, J.D., Minor, E.C., 2008. Absorption spectral slopes and slope ratios as indicators of molecular weight, sources, and photobleaching of chromophoric dissolved organic matter. Limnol. Oceanogr., vol. 53, 955–969.

IPCC 2014. Climate Change 2014: Synthesis Report. Contribution of Working Groups I, II and III to the Fifth Assessment Report of the Intergovernmental Panel on Climate Change / Core Writing Team, R.K. Pachauri and L.A. Meyer (Eds.). IPCC, Geneva, Switzerland, 151 pp.

Jerlov, N.G., 1968. Optical oceanography. Elsevier, Amsterdam, 194 pp.

Kalle, K., 1939. Color of the sea, in: Proc. of the Intern. Council for the Exploration of the Sea. P.V. Rappet (Ed.). No. 109, pp. 98–105. (in German)

Kalle, K., 1966. The problem of gelbstoff in the sea. Oceanogr. Mar. Biol. Annu. Rev., No. 4, 91–104.

Khomutov, A.V., Dvornikov, Yu.A., Gubarkov, A.A., Mullanurov, D.R., 2016. Activation of thermal denudation under recent climatic fluctuations, Central Yamal, Russia. Geophys. Res. Abstr. EGU General Assembly, EGU2016-311, (http://meetingorganizer.copernicus.org/EGU2016/EGU2016-311-1.pdf).

Kokelj, S.V., Jenkins, R.E.L., Milburn, D., et al., 2005. The influence of thawing permafrost on the water quality of small lakes across the forest-tundra transition, Mackenzie Delta region, Northwest Territories, Canada. Permafrost and Periglacial Processes, No. 16, 343–353.

Kokelj, S.V., Zajdlik, B., Thompson, M.S., 2009. The impacts of thawing permafrost on the chemistry of lakes across the subarctic boreal-tundra transition, Mackenzie Delta region, Canada. Permafrost and Periglacial Processes, No. 20, 185–199, DOI: 10.1002/ppp. 641.

Kutser, T., Pierson, D., Kallio, K., et al., 2005. Mapping lake CDOM by satellite remote sensing. Remote Sensing of Environ. 94 (4), 534–540.

Laurion, I., Vincent, W.F., Lean, D.R.S., 1997. Underwater ultraviolet radiation: development of spectral models for northern high latitude lakes. Photochem. Photobiol., No. 65, 107–114.

Leibman, M.O., 2004. Mechanisms of formation of cryogenic translational landslides and conditions for their indication by high willow shrubs on Central Yamal, in: Transactions of the Moscow Center of Russian geographical society. Biogeography, Issue 12, 89–94. RASHN, Moscow. (in Russian)

Leibman, M.O., 2005. Cryogenic slope processes and their geoecologic consequences under the tabular ground ice distribution. Doctor of Sci. (in geol.-mineral.) dissertation, Tyumen, 262 pp. (in Russian)

Leibman, M.O., Kizyakov, A.I., 2007. Cryogenic landslides of the Yamal and Yugorsky Peninsulas. Tip. Rosselkhozakademii, Moscow, 206 pp. (in Russian)

Leibman M.O., Khomutov A.V., Gubarkov A.A., et al., 2015. The research station "Vaskiny Dachi", Central Yamal, West Siberia, Russia – A review of 25 years of permafrost studies. Fennia, No. 193 (1), 3–30.

Parmuzin, S.Yu., Sukhodolskii, S.E., 1982. Massive ground ice in central part of Yamal and its role in the relief formation, in: Plkastovye ldy kriolitozony (Massive ground ice of permafrost zone). IM SO AN SSSR, Yakutsk, pp. 51–61. (in Russian)

Rebristaya, O.V., Khitun, O.V., 1998. Botanical-geographic specifics of the Central Yamal's flora. Botanical Journal (Botanicheskiy Zhurnal) 83 (7), 37–52.

Romanenko, F.A., 1999. Lake basins dynamics on Central Yamal, in: Erozionnye protsessy tsentralnogo Yamala (Erosional processes of Central Yamal). Izd-vo Gomel. TsNTDI, SPb, 350 pp. (in Russian)

Romanovsky, V., Smith, S., Christiansen, H., 2010. Permafrost thermal state in the polar Northern Hemisphere during the International Polar Year 2007–2009: a synthesis. Permafrost and Periglacial Processes, No. 21, 106–116.

Skopintsev, B.A., 1950. Organic matter in natural waters (water humus). Tr. GOIN, 17 (29), 290 pp. (in Russain)

Thompson, M.S., Kokelj, S.V., Wrona, F.J., Prowse, T.D., 2008. The impact of sediments derived from thawing permafrost on tundra lake water chemistry: An experimental approach, in: Proc. of the Ninth Intern. Conf. on Permafrost. D.L. Kane, K.M. Hinkel (Eds.), Fairbanks Alaska, Inst. of Northern Eng., Univ. of Alaska Fairbanks, vol. 2, pp. 1763–1768.

Trofimov, V.T. (Ed.), 1975. The Yamal Peninsula. MGU, Moscow, 278 pp. (in Russian)

Twardowski, M.S., Boss, E., Sullivan, J.M., Donaghay, P.L., 2004. Modeling the spectral shape of absorbing chromophoric dissolved organic matter. Mar. Chem., vol. 89, 69–88.

Twardowski, M.S., Donaghay, P.L., 2001. Separating in situ and terrigenous sources of absorption by dissolved material in coastal waters. J. Geophys. Res., No. 106, 2545–2560.

Ukraintseva, N.G., 1998. Peculiarities of distribution of shrubby tundra on Yamal, in: Transactions of the Moscow Center of Russian Geographical Society. Biogeography, Issue 7, 46–53. RASHN, Moscow. (in Russian)

Vincent, W.F., Laurion, I., Pienitz, R., 1998. Arctic and Antarctic lakes as optical indicators of global change. Ann. Glaciol., vol. 27, 691–696.

Vincent, W.F., Pienitz, R., 1996. Sensitivity of high-latitude freshwater ecosystems to global change: Temperature and solar ultraviolet radiation. Geoscience Canada, vol. 23, 231–236.

Vonk, J.E., Mann, P.J., Davydov, S., et al., 2013. High biolability of ancient permafrost carbon upon thaw. Geophys. Res. Lett., No. 40, 2689–2693, DOI: 10.1002/grl.50348.

Wetzel, R.G., 2001. Limnology: Lake and River Ecosystems. Academic Press, San Diego, USA, pp. 731–759.

Zaneveld, J.R.V., 1975. Penetration of ultraviolet radiation into natural waters, in: Impacts of Climatic Change on the Biosphere. Dept. of Transportation Climatic Assessment Program, Monogr., No. 5, pp. 2-108–2-166.

Zhang, T., Osterkamp, T.E., Stamnes, K., 1997. Effects of climate on the active layer and permafrost on the North Slope of Alaska, U.S.A. Permafrost and Periglacial Processes, No. 8 (1), 45–67.

Zhang, Y., 2004. Highlight article: understanding image fusion. Photogrammetric Eng. and Remote Sensing, No. 70 (6), 657–661.

Received May 2, 2016